

# A High-Performance Doubly-Balanced Mixer in 0.35- $\mu\text{m}$ CMOS for Mode-1 MB-OFDM UWB Receivers

Farid Touati · Skander Douss · Mourad Loulou

Published online: 21 December 2007  
© Springer Science+Business Media, LLC. 2007

**Abstract** A new design of CMOS doubly-balanced down-conversion mixer intended for Multiband Orthogonal Frequency Division Multiplexing (MB-OFDM) receiver of UWB group#1 bands and optimized for 0.35- $\mu\text{m}$  technology is presented. The proposed mixer uses the current-bleeding technique in both the driver and switching stages with wideband impedance matching, consisting of a bandpass filter embedding the RF stage. The mixer performances are optimized for the AMS 0.35  $\mu\text{m}$  CMOS process parameters. Over 3.1–4.8 GHz, the circuit drawing 6 mA from 3-V supply, shows a conversion gain of  $14.0 \pm 1.0$  dB, IIP3 of  $0 \pm 2$  dBm, doubly-sideband noise figure of 4.5–4.8 dB, and port-to-port isolation above 61.0 dB.

**Keywords** Down-conversion mixer · MB-OFDM UWB · Noise figure · Current bleeding · Wideband matching

## 1 Introduction

The rules defined by FCC, for marketing and operation of UWB products, permitted the appearance of other alternatives than the traditional impulse radio technology. Multiband Orthogonal Frequency Division Multiplexing (MB-OFDM), which is an OFDM specification for UWB, has been stressed. After IEEE P802.15 TG3a has been withdrawn, the MB-OFDM specification is under control by ECMA International. ECMA standard [1]

---

F. Touati (✉)  
Department of Electrical and Computer Engineering, Sultan Qaboos Univeristy, Al-Khod, Muscat, Oman  
e-mail: touatif@squ.edu.om

S. Douss · M. Loulou  
Laboratoire d'Electronique et des Technologies de l'Information, National School of Engineering of Sfax,  
B.P. 3038, Sfax, Tunisia  
e-mail: skandar.douss@tunet.tn

M. Loulou  
e-mail: mourad.loulou@ieee.org

specifies the physical and MAC layers. We distinguish two MB-OFDM schemes: the time-frequency interleaving (TFI-OFDM) and fixed-frequency interleaving (FFI-OFDM). In TFI-OFDM approach, information is encoded in 528-MHz-wide bands using 122 QPSK or Dual-Carrier Modulation (DCM) sub-carriers. A frequency hopping scheme is employed, and a variable throughput from 53.3 to 480 Mb/s is provided.

The maximum transmitted power allowed by the FCC in this band is around  $-41.3$  dBm/MHz (i.e., 75 nW/MHz), which is similar to the power from unintentional radiators (TV, PC monitors, etc.). For this reason, receiver blocks need to have high signal amplification.

In a UWB MB-OFDM receiver, a lot of trade-offs are posed in a mixer design. First, the mixer has to meet wideband requirements over the ‘Mode 1’ band. An adequate input matching is then required. The basic trade-off is between gain and linearity. For a high gain, the linearity is less and vice-versa. The current bleeding technique, firstly proposed by Lee and Choi [2], allows improving simultaneously gain and linearity in the case of narrow band ( $f_{RF} = 900$  MHz) single balanced mixers. The same technique was then used in [3] with the doubly balanced mixer topology for an operation from 1.056 to 1.584 GHz only.

This work proposes a TFI-MB-OFDM down-conversion doubly-balanced Gilbert cell mixer that provides high and flat conversion gain and IIP3, low noise figure, and high port-to-port isolation over all UWB bands of group #1, and using the AMS CMOS 0.35  $\mu$ m process parameters.

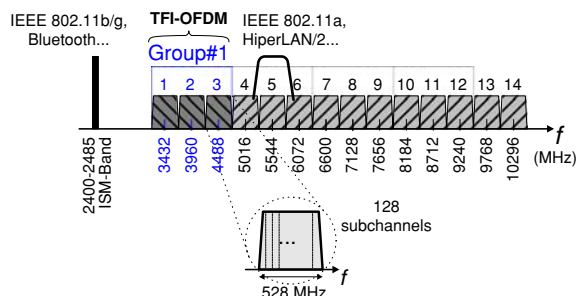
## 2 UWB MB-OFDM Transceiver Architecture

The TFI-OFDM technique is deployed only in the first group of bands from 3.1 to 4.8 GHz (Mode 1) as shown in Fig. 1. The bands are centered at 3.432, 3.960, and 4.488 GHz. This group is mandatory, while all the other groups are for future use (optional). This would allow a CMOS implementation and avoid problems of filtering nearby interferers, e.g., wireless LAN signals in the 2.4–2.5 GHz, WCDMA spurs in the 1–12.75 GHz, cellphones in the 1–2 GHz, and other narrowband interferers in the 2.4–2.5 GHz ISM band [4].

After each OFDM symbol, appending a guard interval provides sufficient time (9.5 ns) to allow both the transmitter and receiver to switch from one band to another. This allows TFI-OFDM to use only one transmitter and one receiver chain at all times.

The down-conversion architecture of the receiver, shown in Fig. 2, is proposed to increase the integration level and hence foster SoC trend [5]. This scheme eliminates many bulky and expensive off-chip components such as image-rejection (no images) and channel-select filters [1]. As a result, this reduces the manufacturing cost, the power consumption, and improves circuit integration. The quadrature down-conversion mixer follows the LNA. Here, the LNA

**Fig. 1** Frequency allocation of MB-OFDM UWB channels



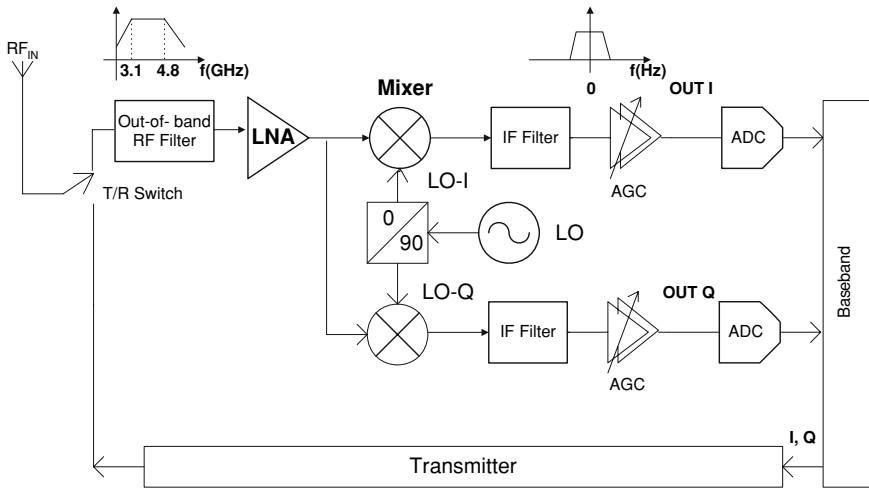


**Fig. 2** Simplified multi-band UWB receiver

and mixer must show wideband characteristics over the band of interest. In fact, these blocks dominate the system linearity, noise performance and determine performance requirements of their adjacent blocks. The variable-gain amplifier (VGA) is connected to the mixer to adjust the signal magnitude [6].

### 3 Design Optimization of 0.35 $\mu$ m CMOS Mixer

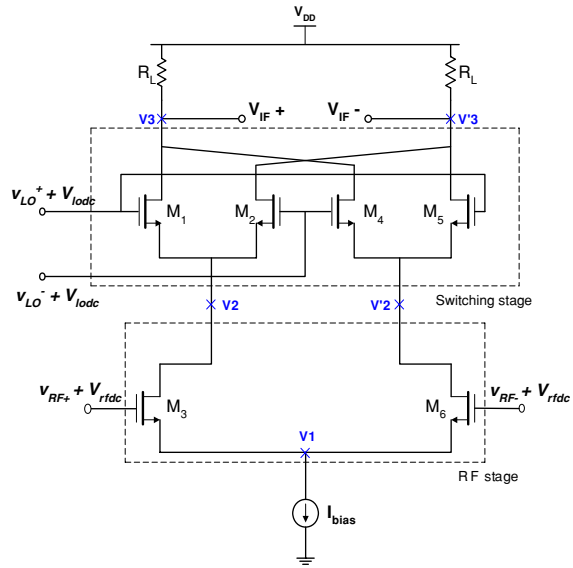
The doubly-balanced active mixer allows for a high conversion gain and eliminates to a great extent the LO signal and even-order distortion products at the mixer output. In addition, a high conversion gain helps in reducing the effects of amplitude and phase mismatch of the LO-I and LO-Q, which degrades the QPSK BER. The current-bleeding technique has proved effective in optimizing trade-offs in mixer design [7]. A uniform response over almost 1.7 GHz bandwidth (3.1–4.8 GHz) requires a wideband RF input impedance matching, which would be hard using a simple inductive degeneration.

In this work, the Gilbert-cell topology was adopted and the dual current bleeding technique (LO and RF bleeding) was used [8]. In single-balanced architectures, the LO noise floor can significantly increase the mixer noise figure. The LO noise floor comprises the noise floor of LO output spectrum plus thermal noise of the polysilicon gate resistance of the switching pairs. The Gilbert-cell topology rejects the external noise present at the LO port and only remains the polysilicon gate resistance thermal noise.

#### 3.1 Active Doubly-Balanced Topology

Because of the low power of the received signal, LNA and mixer must produce a lot of gain all over the 3.1–4.8 GHz band. For this reason, an active mixer is generally adopted. A critical step in mixer design for Gigahertz operation is optimization of device sizing. Figure 3 shows the standard Gilbert cell without the bleeding sources. Resistive loads are used since resistors do not generate flicker noise.

**Fig. 3** Doubly-balanced Gilbert-type mixer structure



In order to determine the range of widths of transistors that would allow covering the 3.1–4.8 GHz group#1 band with a maximum gain using the 0.35- $\mu\text{m}$  process parameters, the mixer conversion gain was simulated for different values of widths. We found that only widths in the 100–200  $\mu\text{m}$  range give acceptable operation in the band of interest. Smaller or bigger sizes either do not give enough gain or unable to operate at high frequencies. For widths in the 100–200  $\mu\text{m}$  range, the maximum conversion gain obtained was around 8.0 dB, which needs to be boosted using circuit techniques.

### 3.2 Input Matching

To improve mixer performances uniformly across the band, RF input impedance matching networks are used.

Two topologies of impedance matching were used; the L-matching and the bandpass filter matching.

#### 3.2.1 L-Matching

In Fig. 4, an L-matching scheme is used at the input of the RF stage and insured by  $L_m$  and the gate-source capacitance  $C_{gs}$  of the RF transistors  $M_{RF1}$  and  $M_{RF2}$ .

Theoretically  $L_m$  and  $C_{gs}$  are given by:

$$L_m \approx \frac{Q \cdot R_s}{\omega_0} \tag{1}$$

$$C_{gs} \approx \frac{Q}{R_s \cdot \omega_0} \tag{2}$$

**Fig. 4** Conventional doubly-balanced Gilbert cell mixer with L-input matching

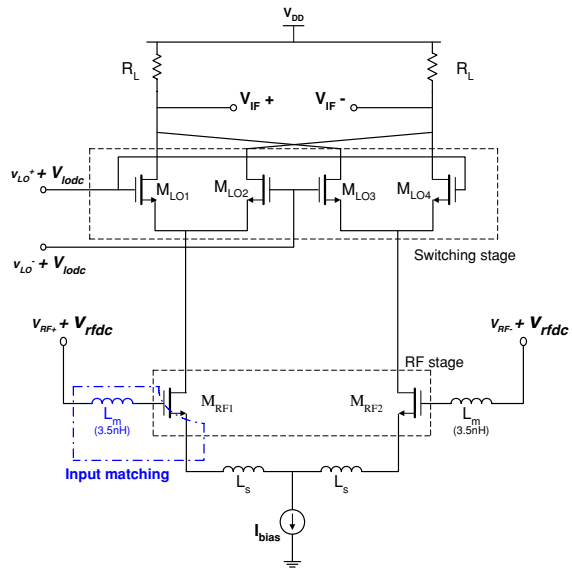
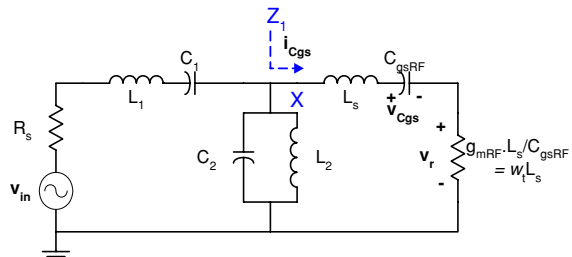


**Fig. 5** Passband matching network



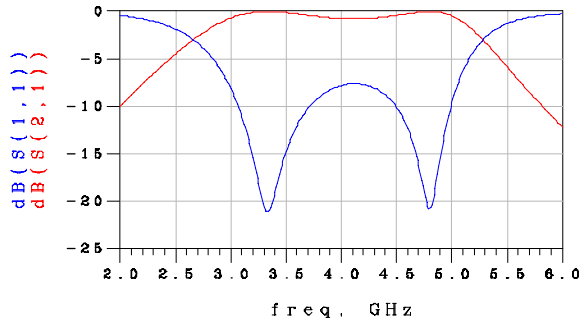
where  $R_s (= 50\Omega)$  is the source resistance,  $\omega_0 = 2\pi f_c$  and  $Q = \frac{f_c}{\text{BW}}$  is the quality factor with BW the band-width and  $f_c$  ( $\sim 4\text{GHz}$ ) is the central frequency of the band of interest. This leads to  $C_{gs} \approx 1.5\text{pf}$  and  $L_m \approx 3.7\text{nH}$ , which is realizable monolithically. The value of  $C_{gs}$  is essentially depending on geometric size of the RF stage transistors. Simulation results showed that the S11 parameter of the matching network is close to 0 dB around the central frequency of 4GHz but not flat over the band of interest.

### 3.2.2 Bandpass Filter Matching

The matching network, shown in Fig. 5, consists of a third-order Chebyshev bandpass filter embedding the RF input stage. This high-order filter stop any intermodulation distortion harmonics that may reach the mixer. The parameter  $C_{gsRF}$  is the gate-source capacitance of the RF input transistor. The values of the different elements were optimized to get a matching over the whole 3.1–4.8GHz band.

Figure 6 shows the S-parameters of the filter, where the output is taken across  $C_{gsRF}$ . As can be seen, an acceptable matching could be reached over the desired band.

**Fig. 6** Frequency response of the input bandpass filter



### 3.3 Current Bleeding Features with L-Matching

Since in the conventional Gilbert Cell mixer, the RF devices operate in the saturation region, the conversion gain (CG) and IIP3 can be approximated by:

$$CG \approx \frac{2}{\pi} R_L \sqrt{K_n \cdot I_{dsRF}} \tag{3}$$

$$IIP3 \approx 4 \sqrt{\frac{2}{3} \frac{I_{dsRF}}{K_n}} \tag{4}$$

with  $R_L$  is the load resistance,  $I_{dsRF}$  is the drain current of the RF stage transistors,  $K_{nRF} = 2\mu_n C_{ox} \frac{W}{L}$  where  $C_{ox}$  is to gate oxide capacitance,  $W$  and  $L$  are, respectively, the width and length of the RF transistors.

Therefore, the IIP3 and the conversion gain are proportional to the square root of the bias current. Consequently, it appears that the mixer performance in terms of linearity and gain can be simply improved by increasing the bias current.

Figure 7 shows a proposed doubly-balanced Gilbert-type mixer with bleeding technique and L-matching network. The p-channel transistors  $M_{BLD1}$  and  $M_{BLD2}$  are used as bleeding current sources. The inductance  $L_1$  is used to increase linearity and decrease the  $1/f$  noise [7,9].

Without  $I_{BLD}$ , the total bias current is:

$$I_{dsRF} = I_{D1} + I_{D2} \tag{5}$$

With  $I_{BLD}$ , it becomes possible to increase  $I_{bias}$  without varying  $I_{D1}$  or  $I_{D2}$ :

$$I_{dsRF} = I_{D1} + I_{D2} + I_{BLD}. \tag{6}$$

This would improve linearity and conversion gain at the same time.

First, to verify that the circuit in Fig. 7 is operating as expected, simulations are performed using ADS software. Figure 8 shows the output signal spectral, where  $f_{RF} = 3.100$  GHz,  $f_{LO} = 3.055$  GHz. This should result in a down-converted signal at 45 MHz.

As can be seen, two frequencies are obtained:

- Up-conversion ‘m2’ (undesired signal) :

$$f_{UP} = f_{RF} + f_{LO} = 6.155 \text{ GHz}$$

- Down-conversion ‘m1’ (desired signal) :

$$f_{DOWN} = f_{RF} - f_{LO} = 45 \text{ MHz}$$

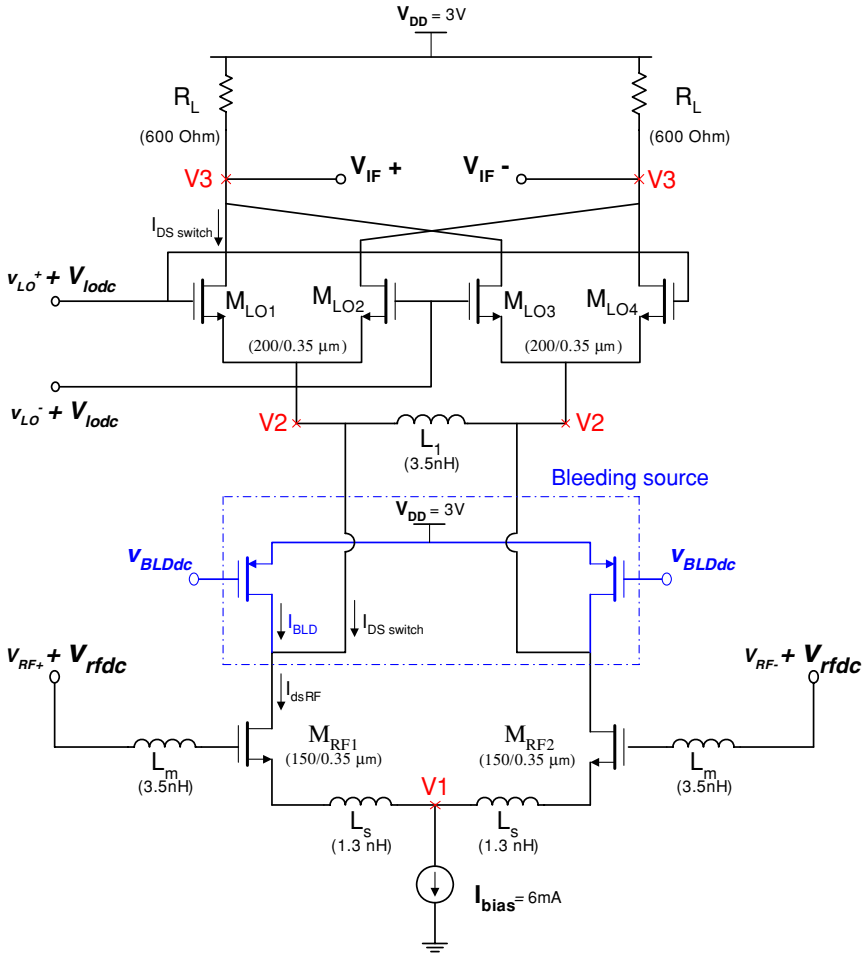
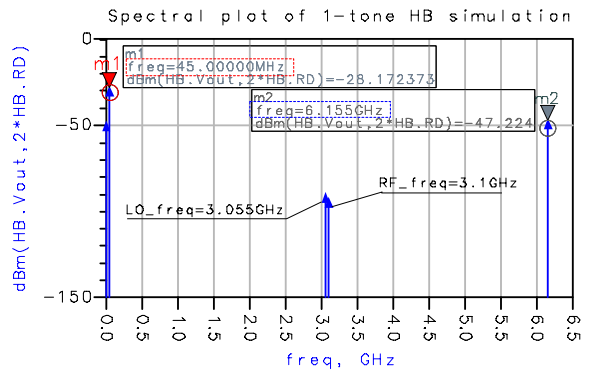
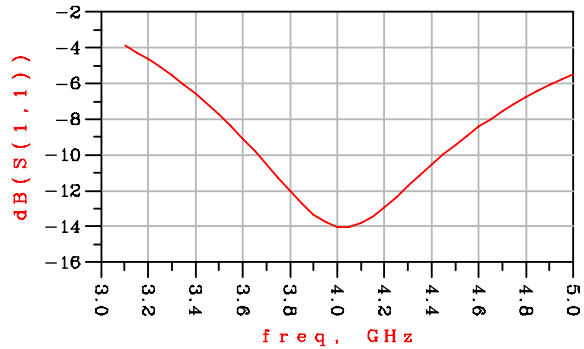


Fig. 7 The UWB doubly-balanced mixer with current-bleeding sources

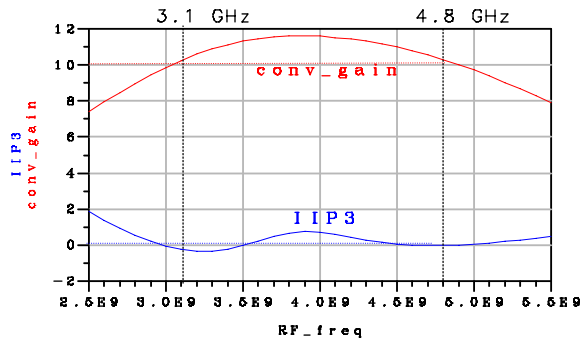
Fig. 8 Simulated mixer output spectrum



**Fig. 9** Simulated S11 trace



**Fig. 10** Simulated conversion gain and IIP3



Consistent results are obtained for the entire band, which is in line with the theory.

Similar results were also obtained with the bandpass filter matching scheme.

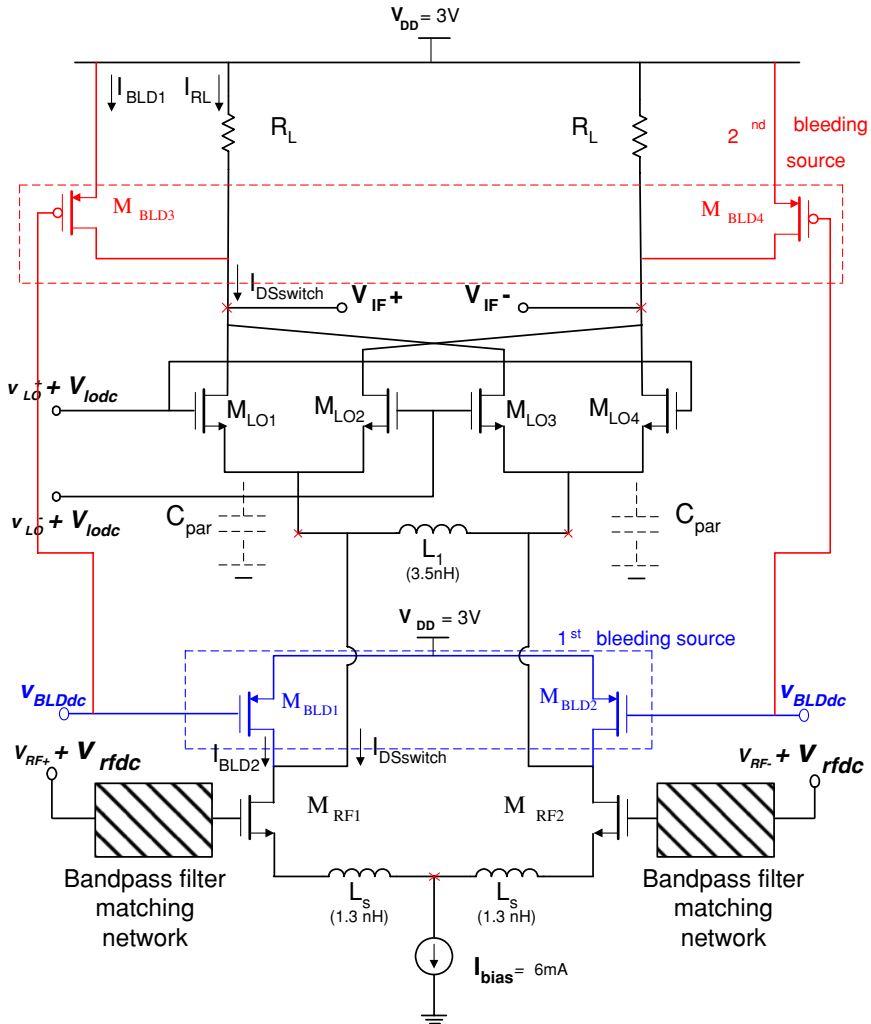
Figure 9 shows the simulated S11 (dB) parameter of the circuit in Fig. 7. The circuit is optimized to provide an input return loss greater than  $-4$  dB. A better input return loss could be achieved with the used L-matching. However, this was at the expense of other performances such as noise figure and linearity. This is because input impedance optimized for gain is not optimum for noise figure for example and vice-versa.

Figure 10 shows the simulation results of the conversion gain and the IIP3 for  $f_{DOWN} = 45$  MHz. A conversion gain above 10 dBm and an IIP3 of about 0 dBm are obtained for the whole band of interest from 3.1 to 4.8 GHz.

As compared to the conventional doubly-balanced mixer in Fig. 3, simulations showed that the bleeding technique allowed an increase of about 2 dBm in the power conversion gain and more than 4 dBm in the IIP3, without degrading the other performances. This topology resolves to a good extent the trade-off between gain and linearity.

### 3.4 An Improved Topology: RF-LO Current Bleeding Doubly-Balanced Mixer

Figure 11 shows the mixer circuit in Fig. 3, where both the LO and RF stages are current-bleeded along with the wideband matching using the bandpass filter matching network in Fig. 5. Also, the driver and switching pairs are degenerated using the inductors  $L_s$  and  $L_1$ , respectively. PMOS transistor pairs ( $M_{BLD1}$ ,  $M_{BLD2}$ ) and ( $M_{BLD3}$ ,  $M_{BLD4}$ ) constitute the bleeding sources for the driver and switching stages, respectively. With the bleeding technique, the current through the switching transistor is reduced, such that the  $1/f$  noise is improved and the output load resistance is increased leading to a higher gain [7, 10]. Also,



**Fig. 11** Mixer circuit with RF and LO current bleeding technique and bandpass filter impedance matching

the bias current through the driver stage can be increased without increasing the current through the switching transistors and vice-versa. This gives more degree of freedom to optimize overall performances of the design than bleeding the driver stage alone.

The conversion gain and IIP3 are also given by (3) and (4), respectively.

The noise sources of a standard Gilbert-cell mixer (Fig. 3) are the driver stage, switching pairs, LO port, and load resistor. The single-sideband (SSB) noise figure due to the contribution of these sources is given by [11]

$$NF_{SSB} = 10 \log \left[ \frac{\alpha}{c^2} + \frac{2(\gamma_{RF} + r_{gRF}g_{mRF})\alpha g_{mRF} + 4\gamma_{LO}\bar{G} + (4r_{gLO})\bar{G}^2 + \left(\frac{1}{R_L}\right)}{R_s c^2 g_{mRF}^2} \right]. \tag{7}$$

**Fig. 12** Simulated conversion gain and IIP3

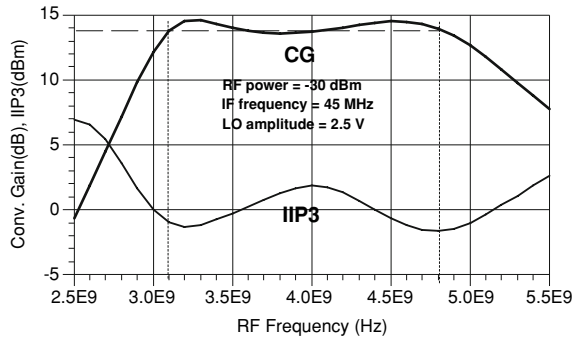
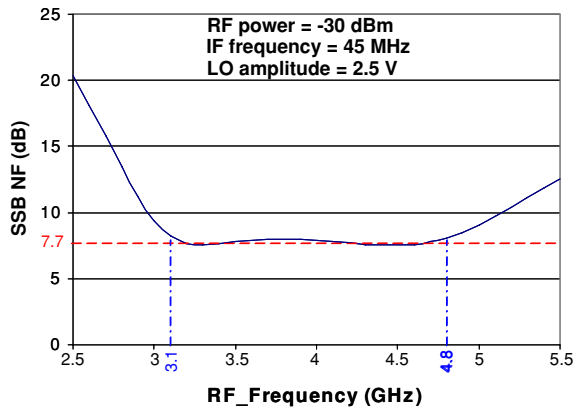


**Fig. 13** Simulated single-sideband noise figure



In (7),  $\alpha$  and  $c$  (the conversion gain of the switching pair alone) are parameters depending on the LO signal waveform. For large LO amplitudes, the LO signal approaches a square waveform. In this case,  $\alpha$  approaches 1 and  $c$  approaches  $2/\pi$ . The parameter  $T$  in (7) is the absolute temperature,  $R_s$  is the input source resistance which drives the mixer RF port,  $g_{mRF}$  and  $g_{mLO}$  are the instantaneous small-signal transconductances of RF and LO transistors, respectively,  $r_{gRF}$  and  $r_{gLO}$  their polysilicon gate resistances, and coefficient  $\gamma_{RF}$  and  $\gamma_{LO}$  are equal to  $2/3$  for long channel and higher for submicron transistors. The parameter  $\bar{G}$  is the time average of  $G(t)$ , the small-signal transconductance of the whole LO differential pair. The doubly-sideband noise figure is 3-dB less than that of the single-sideband in (7).

Figure 12 shows the simulated conversion gain and two-tone IIP3 test results of the circuit in Fig. 11 as a function of RF frequency with an LO frequency 45 MHz apart so that a baseband signal at 45 MHz is observed. The bandpass filter matching scheme is used. The RF power and LO voltage amplitude were fixed at  $-30$  dBm and 2.5 V, respectively. The corresponding SSB noise figure is shown in Fig. 13. These curves were optimized for the 0.35- $\mu$ m process parameters. The average conversion gain is 14.0 dB and varies only  $\pm 1$  dB across the bandwidth. This relaxes the requirement for baseband gain compensation to recover a flat conversion gain curve. Usually, this compensation degrades the noise figure. The IIP3 is  $\pm 2$  dBm around 0.

The SSB noise figure is flat at about 7.7 dB. The DSB-NF would be 3-dB less and hence around 4.7 dB. The current bleeding transistors in Fig. 11 were optimized to make their contribution to the total noise figure and linearity marginal. The inductor L1 improves the noise figure, conversion gain, and linearity by increasing the commutation bandwidth of the

**Fig. 14** Dependence of output power on the input RF power

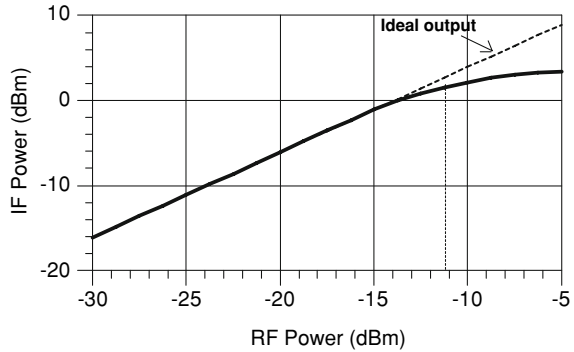


**Table 1** Simulated port-to-port isolation for IF frequency = 45 MHz, RF power = -30 dBm and LO amplitude of 2.5 V

UWB group#1 band	LO frequency (GHz)	LO-IF (dB) $\geq$	RF-IF (dB) $\geq$	LO-RF (dB) $\geq$
1	3.387	-66.0	-62.0	-69.0
2	3.915	-72.0	-66.0	-66.0
3	4.443	-79.0	-64.0	-61.0

switching devices through entirely or partially tuning out the parasitic capacitance in the switching pairs tail current  $C_{par}$ . An optimum value of  $L1$  was 3.3 nH, which can be on-chip. With this value of  $L1$ , the overall noise figure was improved by about 2.2 dB for downconverted frequencies above 1 MHz.

Compared to those obtained for circuit with L-matching scheme and RF stage current-bleeding (Fig. 7), the above results show that the RF and LO current bleeding, employed here, have a great effect in improving the conversion gain while marginally degrading other performances.

Figure 14 shows the mixer power performance when the RF frequency is 3.960 GHz, corresponding to the center of second band of group#1. The IF frequency is set to 45 MHz. The 1-dB compression point ( $IP_{1dB}$ ) attained is -11.2 dBm. Similar values were obtained for bands #1 and #3.

The intrinsic performance of the port-to-port isolation in a fully balanced Gilbert mixer is maintained. We found that the bleeding current sources have no effect on the port-to-port isolation. As shown in Table 1, the simulated LO-to-IF, LO-to-RF, and RF-to-IF isolations are better than -66, -61, and -62 dB, respectively, for LO frequencies 45 MHz offset from the RF frequencies over all the three bands of group#1. The RF power was maintained at -30 dBm and the LO amplitude at 2.5 V.

The high LO-to-RF isolation indicates that the self-mixing problem, and hence the dc offset at the mixer output, is small enough not to affect output voltage headroom. We noticed that the matching network degraded these isolations by about 5.0 dB, which is relatively marginal. The high isolations levels achieved here are as or better than those proposed in the literature using sub-harmonic mixer topologies based on the doubly-balanced structure [12].

Table 2 summarizes the performances of the proposed design in Fig. 11. The conversion gain,  $IP_{1dB}$ , IIP3, DSB-NF, and port-to-port isolation are in the same range in all UWB channels in group#1.

**Table 2** Summary of simulated performances for IF frequency = 45 MHz, RF power = -30 dBm (variable for the IP1 dB and IIP3), and LO amplitude = 2.5 V

UWB group#1 band (GHz)	Gain (dB)	IP <sub>1</sub> dB (dBm)	IIP3 (dBm)	DSB-NF (dB)	Power (mW)	Port-to-port Isolation
3.432	14.2	-11.3	-0.7	4.5	18.0	≥62.0
3.960	13.7	-11.2	+1.8	4.5	18.0	≥66.0
4.488	14.3	-12.5	-0.7	4.8	18.0	≥61.0

The proposed idea of wideband input matching using a bandpass filter, mixed with dual (RF and LO) current bleeding proves to be very effective in attaining uniform wideband performances because the achieved figures are better than in solutions where these techniques were not used.

#### 4 Conclusion

A 3.1–4.8-GHz CMOS down-conversion doubly-balanced mixer for time-frequency interleaving MB-OFDM receiver front-end was presented. The mixer conversion gain, linearity, noise performance, and port-to-port isolations were discussed. What is notable is the uniformity of these parameters across all bands. This was achieved by combining the use of bleeding technique along with wideband impedance matching of the driver stage over the entire band. Bleeding both the driver and switching stages was used for the first time to allow better optimization of trade-offs. Over 3.1–4.8 GHz, the circuit drawing 6 mA from 3-V supply, shows a conversion gain of  $14.0 \pm 1.0$  dB, IIP3 of  $0 \pm 2$  dBm, doubly-sideband noise figure of 4.5–4.8 dB, and port-to-port isolation above 61.0 dB. Inductively degenerating the switching pairs allowed reducing the overall noise figure by about 2.2 dB when downconverted frequencies are above 1 MHz. The intrinsic performance of the port-to-port isolation in a fully balanced Gilbert mixer was not degraded. The idea of mixing wideband matching of RF input with dual current-bleeding technique proved interesting in improving the performance and uniformity over all UWB bands of group#1.

#### References

1. ECMA (2005). Standard ECMA-368: High rate ultra wideband PHY and MAC standard. December, 2005.
2. Lee, S. G., & Choi, J.-K. (2000). Current-reuse bleeding mixer. *Electronics Letters*, 36, 696–697.
3. Phan, A. T., Kim, C. W., Shim, Y. A., & Lee, S. G. (2005). A high performance CMOS direct down conversion mixer for UWB system. *IEICE Transactions Electronics*, E88, 4372–4380.
4. Gharpurey, R. (2005, June). Design challenges in emerging broadband wireless systems. Paper Presented at IEEE Radio Frequency Integrated Circuits (RFIC) Symposium. Digest of Technical Papers, pp. 331–334.
5. Ismail, A., & Abidi, A. A. (2005). A 3.1–8.2 GHz Zero-IF receiver and direct frequency synthesizer in 0.18  $\mu$ m SiGe BiCMOS for mode-2 MB-OFDM UWB communication. *IEEE Journal of Solid-State Circuits*, 40(12), 2573–2582.
6. Sung, C.-C., Chou, M.-F., Wu, C.-C., Chen, C.-S., Wen, K.-A., & Chang, C.-Y. (2004, December). Low power CMOS wideband receiver design. Paper Presented at The 16th International Conference on Microelectronics, ICM'2004, pp. 287–290.
7. Lee, S.-G., et al. (2000). Current-reuse bleeding mixer. *Electronics Letters*, 36(8), 6960–6967.
8. Touati, F., Douss, S., & Loulou, M. (2007, February). A 3.1–5 GHz CMOS active mixer for UWB IEEE 802.15.3a standard receivers. Paper Presented at the International Conference on Communication, Computer and Power ICCCP'07, pp. 6–10.

9. Park, J., Lee, C.-H., Kim, B.-S., & Laskar, J. (2006). Design and analysis of low flicker-noise CMOS mixers for direct-conversion receivers. *IEEE Transactions on Microwave Theory and Techniques*, 54, 4372–4380.
10. Darabi, H., & Abidi, A. A. (2000). Noise in RF-CMOS mixers: A simple physical model. *IEEE Journal of Solid-State Circuits*, 35(1), 15–25.
11. MacEachern, L. A., & Manku, T. (1998, May). A charge-injection method for Gilbert cell biasing. Paper Presented at IEEE Canadian Conference on Electrical and Computer Engineering, pp. 365–368.
12. Wu, T.-H., Tseng, S.-C., Meng, C.-C., & Huang, G.-W. (2007). GaInP/GaAs HBT sub-harmonic Gilbert mixers using stacked-LO and leveled-LO topologies. *IEEE Trans. Microwave Theory and Techniques*, 55(5), 880–889.

## Author Biographies



**Farid Touati** has over ten years' experience designing electronic systems for conventional and hard-environment applications in communications, telemetry, and signal processing. Following the completion of his PhD in Electrical Engineering at Nagoya Institute of Technology of Japan in 1995, he worked at Universities in Japan, Saudi Arabia, and the US. He is currently employed as a Professor at Sultan Qaboos University of Oman.



**Skandar Douss** was born in Ksar Hellal, Tunisia in 1979. He received the Electrical Engineering Diploma then the Master degree in electronics from the National School of Engineering of Sfax "ENIS", respectively, in 2003 and 2004. He joins the Electronic and Information Technology Laboratory of Sfax "LETI" since 2003 and he has been a PhD student at the National School of Engineering of Sfax "ENIS" from 2004. His current research interests are on analogue RF CMOS integrated circuits design.



**Mourad Loulou** was born in Sfax, Tunisia in 1968. He received the Engineering Diploma from the National School of Engineering of Sfax in 1993. He received his Ph.D. degree in 1998 in electronics system design from the University of Bordeaux France. He joins the electronic and information technology laboratory of Sfax "LETI" since 1998 and he has been assistant Professor at the National School of Engineering of Sfax from 1999. Since 2004 he has been an associate Professor at the same institution. Actually he supervises the Analogue and Mixed Mode Design Group of LETI Laboratory. His current research interests are on analogue, mixed and RF CMOS integrated circuits design and automation.